

incomplete knowledge of watershed processes or different assumptions during model setup, whereas parameter uncertainty arises due to the availability of validation data, imprecise representation of parameter ranges and distributions. In addition, input uncertainty is generated from simplifications in natural randomness and temporal-spatial data variability and would be inevitably magnified by model uncertainty to larger output errors.

Model inputs typically include spatial data, such as spatial precipitation input, digital elevation models (DEMs), land use maps and soil maps, as well as attribute data, such as fertilizer amount (Shen et al., 2013). The uncertainty of spatial data, typically in the forms of GIS maps, is derived from many factors, including the quantity of available scenes, the resolution for the data that were captured, and the choice of interpolation techniques (Wu et al., 2005). Rainfall plays a crucial role in runoff production and mass transport so its reliability has been considered as major factor for the accuracy of hydrological models. Traditionally, the rain station is the fundamental tool for representing spatial distribution of rainfall within a watershed (Andréassian et al., 2001). Designing the proper location, number and density of rain-gauge stations is important to hydrological research (Duncan et al., 1993). Studies have explored the impact of heterogeneous rainfall data on parameter estimation and model outputs and concluded that large bias could be expected if detailed variations in the rainfall data are not considered (Strauch et al., 2012).

As another important GIS data, a DEM is used to extract surface characteristic parameters, such as watershed boundary, slope, and thus flow direction, so its resolution influences model outputs (Lin et al., 2013; Wellen et al., 2014). Studies have noted that coarser DEMs smooth watershed slope and thereby reduce the simulated peak flow or sediment yields (Zhang et al., 2014). It is also shown that nitrogen output decreased with the decreased DEM resolution, while a decreased DEM resolution does not always result in decreased total phosphorus (TP) (Chaubey et al., 2005). In this sense, the question about whether higher-resolution data would always lead to better model performance should be considered first (Shen et al., 2013). In the meantime, GIS

11423

data may be available from alternative sources; therefore, another question is which specific data set should be used. For example, land use maps could be obtained from federal, state and local government agencies, whereas county and local governments are developing detailed datasets (Shen and Zhao, 2010; Han et al., 2014). Land use maps for a specific point in time, typically obtained by interpreting remote sensing data, are often used, and possible changes in land uses during that specific period are not considered (Mango et al., 2011; Pai and Saraswat, 2013).

Despite the research progress described above, input-induced uncertainty remains a significant challenge due to various input data, which largely limits the applicability of watershed models. For example, model-based programs, such as Total Maximum Daily Loads (TMDLs), are often criticized for their inadequate consideration of input uncertainty (Chen et al., 2012). First, there is relatively more uncertainty research about hydrological processes but less on NPS pollution. Second, the sensitivity of watershed models also depends on how well attribute data aggregation describes the relevant characteristics of human management. Thus, it is useful to understand the assumptions of attribute data and how these assumptions will likely impact the model results. Third, previous studies have not evaluated the relative contribution of each input data set so a strategy on how to reduce input uncertainty cannot be formulated in a cost-effective manner (Munoz-Carpena et al., 2006).

The main objective of this paper is to conduct a comprehensive assessment of input-induced uncertainty in TP modeling. Four key types of input data, i.e., rainfall, topography, land use and fertilizer amount, are analysed, and their uncertainties are quantified. The uncertainties related to these input data are then compared.

11424

2 Materials and methods

2.1 The description of the study area

The Upper Daning River Watershed, which is located in the Three Gorges Reservoir Area of China, was selected as the studied watershed (Fig. 1). This watershed, covering an area of 2421 km², is characterized as being located in a northern subtropical monsoon climate with an annual mean rainfall of 1182 mm (ranging from 761 to 1356 mm). This watershed is very mountainous with elevations ranging from 200 to 2605 m. The primary land uses in this watershed are forest (61.8%), arable land (25.3%), and pasture (12.5%), and yellow-brown earths (26.5%), yellow-cinnamon soils (16.9%) and purplish soils (14.5%) are the dominant soil types. Based on the characteristics of the river system, the studied watershed was broken into six drainage regions: Dongxi river, Xixi river, Baiyang river, upper region of the Wuxi hydrological gauge, Houxu river, and upper region of the county boundary (watershed outlet). As illustrated in Fig. 1, the corresponding outlets of are referred to as DX, XX, BY, WX, HX, and CF, respectively. In this study, TP was evaluated as P was recognized as the key limiting factor of eutrophication in this region.

2.2 Model description

In this study, the SWAT model, as a commonly-used watershed model, was used for NPS-TP modeling. The studied watershed was partitioned into 22 sub-watersheds from a constructed DEM and each sub-watershed is then divided into hydrologic response units (HRUs) by designing their homogeneous slope, soil, and land use. To use the SWAT model efficiently and effectively, the SWAT-CUP software (Abbaspour et al., 2007) was applied for model calibration and validation. The measured water quality and flow data were obtained from the Changjiang Water Resources Commission as well as local government. Thereafter, the SWAT model was calibrated and validated using the initial input data (Shen et al., 2012a), and the transitivity error from input data

11425

to model outputs was quantified by changing the available datasets while keeping the calibrated parameters fixed.

2.3 Generation of input-induced uncertainty

Errors introduced by rainfall data, DEMs and land use maps were analyzed. The influence of soil type maps was not analyzed, because only one soil map data (coarse resolution at 1 : 1 000 000) was available for the study region. These GIS data are the most frequently used in hydrology and NPS modeling in the Yangtze River Watershed and other areas of China. The errors related to fertilizer amount were also investigated due to the lack of detailed farm-scale data.

2.3.1 Spatial data 1: rainfall data

In this study, rainfall datasets were collected from twelve rain gauges located within the watershed boundary and two outside stations that were within approximately 10 km of the watershed boundary were also used (Fig. 1). The rain gauge falling within a given sub-catchment is identified using the GIS software. The annual mean rainfall recorded by these rain gauges is listed in Table 1. Previous studies have demonstrated rainfall uncertainty comes from the lack of representative rain gauges and the need to interpolate the rainfall data between rain gauges (Andréassian et al., 2001; McMillan et al., 2011). In this sense, rainfall data-induced uncertainty was analyzed in two steps: (1) the dataset of each rain gauge was used as inputs for the SWAT model separately, and the model performances were ranked based on the E_{NS} values for single gauge simulations, (2) random combinations of m rain gauges (m ranged from 2 to 12) were generated and used as SWAT inputs. Our previous study (Shen et al., 2012a) has already focused on the impact of interpolation methods on the spatial rainfall heterogeneity; therefore, the expected rainfall spatial distributions were only generated by the chosen density of rain gauges. The centroid method was selected because it

11426

was the current approach incorporated into the current version of SWAT model and the easiest to apply (Shen et al., 2012a).

2.3.2 Spatial data 2: DEMs

In this watershed, two DEM sets were available for NPS modeling: (1) the National Fundamental Geographic Information System of China DEM (NFGIS DEM) and (2) the ASTER GDEM. Specifically, the NFGIS DEM was acquired in 1998 from a topographic map with a resolution of 90 m, whereas the ASTER GDEM was created by a satellite-borne sensor that covered the surface land at a resolution of 30 m (Shen et al., 2013). To study the impact of data resolution on NPS simulations, both DEMs were converted to coarser ones using the resample function of ArcMap. Finally, four NFGIS DEM maps (90 m × 90 m, 120 m × 120 m, 150 m × 150 m and 180 m × 180 m), and ten ASTER GDEM maps (30 m × 30 m, 40 m × 40 m, 50 m × 50 m, 60 m × 60 m, 70 m × 70 m, 80 m × 80 m, 90 m × 90 m, 120 m × 120 m, 150 m × 150 m and 180 m × 180 m) were obtained.

2.3.3 Spatial data 3: land use maps

As discussed above, land use data available for the modeling effort will likely come from numerous sources; therefore, an assessment of available land use data and the time period covered by these data should be made. In this study, land use data were obtained from the 1980s (1980–1989), 1995, 2000, and 2007. The land use statistics are shown in Table 2. Specifically, maps from the 1980s, 1995 and 2000 were interpreted from MSS/TM/ETM images by the Chinese Academy of Sciences, whereas the land use map for 2007 was created from a TM image. In our previous study (Shen et al., 2013), the resolution of land use data was shown to have only a slight influence on simulated NPS-P for the study region; therefore, the land use map was not resampled in this study.

11427

2.3.4 Attribute data: amount of fertilizer

Attribute data, including crop planting time, irrigation, fertilization, and tillage, were mainly obtained from the agricultural bureau and local farmers; therefore, these data only reflect the aggregate information at an average level. In this sense, there were inevitable differences in management practices among farmers; therefore, the use of this average information might result in fertilizer amount errors. In this analysis, the uncertainty due to the amount of fertilizer applied was also treated as input uncertainty. Initially, the annual applied urea and compound fertilizer was set as 450 kg ha⁻¹ and 300 kg ha⁻¹ based on our limited local investigation. Using the Monte Carlo technique, different fertilizer amount datasets were generated by sampling stochastically from a normal distribution expressed as $X \sim N(\mu, \sigma^2)$, where μ and σ are the recorded amount of fertilizer and the standard deviation (SD), respectively. The Latin Hypercube sampling technique, which employs a constrained sampling scheme instead of random sampling, was applied to ensure a sufficient precision of sampling. To cover 99.7% of the error range, the sampling range was designated as ±15% from the initial amount of fertilizer and 5000 model runs were conducted.

2.4 Analysis of the model results

This study focused on error-transitivity from input data to NPS-TP predictions (the sum of organic P and mineral P) at the WX for the period from 2000 to 2007. First, the sensitivity of simulated TP to each input data was quantified in the form of summary statistics, such as the SD and the coefficient of variation (CV). Specifically, the CV, which is a normalized measure of dispersion of a probability distribution, is defined as a dimensionless number by quantifying the ratio of the SD to the MV. Compared to SD, the CV is more appropriate for comparing different data sets; therefore, it was used as the main approach for expressing uncertainty in this study.

11428

$$s = \sqrt{\frac{1}{m} \sum_{j=1}^m (x_j - \bar{x})^2} \quad (1)$$

$$c = \frac{s}{\bar{x}} \quad (2)$$

where s and c represents the SD and the CV, respectively, x_j represents simulated data point j , $\bar{x} = \frac{1}{m} \sum_{j=1}^m x_j$ indicates the mean value of simulated data, and m is the number of simulated data.

To re-validate the range of input data, the Nash–Sutcliffe coefficients (E_{NS}) was used to the accuracy of SWAT outputs.

$$E_{NS} = 1 - \frac{\sum_{i=1}^n (x_{sim,i} - x_{mea,i})^2}{\sum_{i=1}^n (x_{mea,i} - \bar{x}_{mea})^2} \quad (3)$$

where $x_{mea,i}$ and $x_{sim,i}$ is the simulated and measured data for the i th pair, respectively, \bar{x}_{mea} represents the mean value of the measured values, and n is the total number of paired values.

Generally, watershed modeling involves two kinds of uncertainty: (1) systematic model uncertainty regardless of correct input, and (2) uncertainty due to inaccurate input. In this study, model structure was fixed and model results will be dependent on the interaction of input errors. Based on the performance ratings by Moriasi et al. (2007), $E_{NS} \geq 0.5$ was recommended for selecting behavior input datasets though those effective simulations, which refer to the phenomenon of equifinality and can be representative of a watershed system ($E_{NS} \geq 0.5$) (Liu and Gupta, 2007). In the next step, behavior input data ($E_{NS} \geq 0.5$) were grouped in all possible ways to further

11429

constrain the model uncertainty by using a multi-input ensemble method. Finally, input-induced model uncertainty was generated via sampling from the output distributions that are generated from these effective input datasets.

3 Results

3.1 Calibration and validation

As shown in Table 3, for the flow simulation, the E_{NS} were 0.89 and 0.66 in the calibration and validation periods, respectively. The E_{NS} values were 0.73 and 0.67 for sediment during the calibration and validation periods, and 0.75 and 0.46 for TP. More details about the final SWAT parameters can be found in our previous studies (Shen et al., 2012a, 2013). Compared to the SWAT performances complied by Moriasi et al. (2007), the accuracy of flow prediction could be judged as very good, while the sediment and TP simulations were judged to be satisfactory.

3.2 Sensitivity of each input dataset

To determine the sensitivity of each input dataset, the degree of uncertainty of simulated TP was illustrated in Fig. 2. As shown in Fig. 2a, the annual mean CV ranged from 0.284 (2006) to 0.587 (2003), indicating there were significant uncertainties in these single rain gauge simulations. The E_{NS} values for each rain gauge are 0.70 for XN, 0.49 for LM, 0.39 for TF, 0.38 for SY, 0.31 for WX2, 0.07 for WX, 0.06 for WG, 0.02 for XJB, -0.07 for ZL, -0.12 for CA, -0.68 for GL, and -2.87 for JL. This indicates that most of the E_{NS} values were low, especially for ZL, CA, GL and JL because no rainfall data were recorded in these gauges for the period from 2000 to 2003. As shown in Fig. 2b, using data from multiple rain gauges as inputs, the CVs ranged from 0.098 (2006) to 0.433 (2000), suggesting that TP simulations are sensitive to the density of rain gauges. The model performance improved when the number of rain gauges increased from 2 to 5. However, a plateau was reached at approximately 6 gauges.

11430

Using NFGIS DEMs (Fig. 2c), the CV values were found to be low with an annual mean CV of 0.026–0.119, but the CV values were higher using ASTER DEMs (Fig. 2d), with CV values ranging from 0.105 to 0.383. Figure 2e shows the statistical analysis using different land use maps. Compared to the input data presented above, the annual mean CV values, which ranged from 0.009 to 0.036, were relatively low. Besides, as shown in Fig. 2f, the simulated TP showed only slight variation related to the errors in the amount of fertilizer, with mean CV values of 0.003–0.008.

Finally, a multi-input ensemble method was used for a comprehensive evaluation of input-induced model uncertainty. As shown in Table 4, the annual CV values of simulated TP ranged from 0.101 to 0.271, indicating a temporal variation for the period from 2000 to 2007. The ensemble of input-induced outputs was also determined for all six given outlets. As illustrated in Fig. 3, the annual mean CV values were 0.190 for XX, 0.088 for DX, 0.206 for HX, 0.162 for BY, 0.168 for WX and 0.135 for CF.

4 Discussion

4.1 Comparison between different input data-induced uncertainty

Table 4 gives a clear comparison between different types of input data. For the given catchment and rainfall characteristics, rainfall input is identified as the most important factor in NPS simulation, whereas rain gauge density is the most important source contributing to the overall uncertainty. The results from the statistical analysis are reasonable as rainfall is the major driving force of NPS pollution (Andréassian et al., 2001; McMillan et al., 2011). As shown in Table 1, rainfall data varied substantially among different gauges, with a 933 mm difference between the highest and lowest annual rainfalls. This finding agrees with previous research (Strauch et al., 2013) in which the rainfall input was averaged across the watershed by a single rain gauge, but failed to adequately reflect spatial rainfall variations. This can be attributed to the SWAT rule for quantifying the sub-watershed rainfall, in which rainfall data from the

11431

closest gauge is selected as inputs for each sub-watershed. In cases where a sub-watershed contains no rain gauges, the centroid is used to find the nearest gauge and its data are substituted for the sub-watershed rainfall. Another reason might be the use of the same parameter set in all simulations. Bárdossy and Das (2008) found that fewer gauge simulations might produce similar results when compared with those obtained by more rain gauges due to the compensation effect from calibration. However, even with the best calibration process, there is always parameter uncertainty in the model predictions due to the availability of validation data, imprecise representation of parameter ranges and distributions; therefore, recalibration was not conducted in this study (Van Griensven et al., 2006).

Figure 2b illustrates that there were reductions in the CV values compared with the single-gauge simulations, which clearly showed that the ensemble of multi-gauge simulations outperformed the single-gauge simulations. However, no clear relationship existed between the E_{NS} and the rain gauge location, which is also inconsistent with a previous study. Schuurmans and Bierkens (2007) found greater model errors if gauges outside the watershed were used, but this is not the case for the present study because the outside gauges were relatively close (10 km) to the watershed boundary. Figure 2b indicates that the use of these key gauges appear to be more informative in constraining spatial rainfall variations but simulation efficiency did not always improve when additional gauges are added. This demonstrates that the information content in rainfall spatial variation is reached after a relatively small number of key gauges are used as model input (Seibert and Beven, 2009). It is encouraging that a small number of gauges distributed more optimally and perform well for logistical reasons (Bárdossy and Das, 2008; McMillan et al., 2011). In reality, there might not be many dense rain gauge networks similar to those used for this study; therefore, the fact that spatial rainfall variation is a function of key gauges rather than all gauges would indicate a wider range of applicability.

As illustrated in Fig. 2c and d, the second highest uncertainty was caused by DEMs, and the ASTER GDEM-induced uncertainty was higher than by uncertainty induced

11432

by NFGIS DEM. These higher values could be due to the following two reasons: first, NFGIS DEM was already validated in many places in China, which was not the case for ASTER GDEM (Wu et al., 2007; Dixon and Earls, 2009). In fact, ASTER GDEM contains systematic errors; i.e., a significant number of anomalies attributable to cloud disturbances, the algorithm used to generate the final GDEM, and not applying inland water mask. Second, the initial resolution of NFGIS DEM (90 m × 90 m) was lower than that of ASTER GDEM (30 m × 30 m). In reality, those high resolution DEMs might provide better simulations, but sometimes a moderate one would be more suitable due to the nonlinearity of erosion processes and its subsequent effect on P processes (Chaplot et al., 2005). Given the nature of ASTER GDEM, the greater degree of averaging has occurred by adding shallower slopes, and the predicted TP would be lower by increasing more infiltration and deposition of NPS-TP. In this sense, it is important to select a certainty-appropriate data source because DEMs are generated at different scales and a number of the implied watershed processes are scale-dependent (Brazier et al., 2005). Care must be taken in DEMs data resolution because their resolutions cannot be up-scaled directly. In theory, topography exerts some level of control on surface flow and thus NPS loads. Therefore, the smoothing of the landscape shape induced by coarser DEMs could result in a biased estimation of TP outputs (Dixon and Earls, 2009). It was worthwhile to parameterize the SWAT model with the extreme slopes, as these slopes controlled the fluxes of NPS-TP. However, our previous study has also demonstrated that the TP simulations would not be improved if certain resolution was reached (Shen et al., 2013). In this sense, some balance must be found between improving the DEMs resolutions and reducing the complexity of the model utility.

In contrast, land use maps and fertilizer amount resulted in low uncertainties. The result differ from those of Payraudeau et al. (2004), who found that model outputs were highly sensitive to land use changes. This could be explained by the fact that most agricultural land was redistributed to forest and other land uses in the study of Payraudeau et al. (2004), which leads to significant changes in soil compaction and

11433

ground cover. However, these low values in our study could be due to minor land use changes during the period from the 1980s to 2007. As shown in Table 2, the fraction of forest area decreased gradually from 61.75 to 54.76 %, whereas agricultural land increased from 25.68 to 33.47 %. Figure 2f indicates that the fertilizer input has only a slight impact on in-stream TP loads. This was because P application was low in this watershed with the inorganic N being applied in greater amounts and more widely. Additionally, according to the mechanism of the SWAT model, P would be taken up mainly by crop rotation, and this process would govern the turnover rates and transport of P. Therefore, only a small proportion of P will finally flow into the water body as in-stream NPS-TP. In this sense, there might also be minor CV values if other representative attribute practices, e.g., tillage data, were selected. This indicates the degree of sensitivity due to single input data depends on two factors: the ratio of each individual input contribution to the total load (which is the case for management data) and the error in the individual input (which is more meaningful for land use maps).

4.2 Comprehensive evaluation of input data-induced uncertainty

As shown in Fig. 3, this demonstrated that input-induced uncertainty may be highly area-specific; i.e., dependent upon the scale of the drainage area and rainfall variability. For example, when multiple gauges (from 1 to 12) are used as model inputs, the simulated TP remained stable for the DX and no model uncertainty was observed. This could be due to the mechanism of SWAT, in which only the rainfall data from the closest gauge to the centroid were chosen and used as the sole model input for that specific sub-watershed. As shown in Fig. 1, there is only one sub-watershed in the DX region and the XN gauge is closest to its centroid; therefore, the rainfall data from the same gauge was used every time for this region. However, the CV values remained high for other outlets, ranging from 0.187 (CF) to 0.448 (XX), suggesting that rain gauge density indicated different impacts under different spatial scales of drainage areas. In addition, using different DEM data, the CV values were relatively low for XX, DX, WX and CF, with an annual mean CV of 0.022–0.055, but the CV values were relatively high for HX

11434

and BY, with values of 0.152 and 0.136, respectively. This could be explained by the fact that there are more mountainous areas along XX, DX, WX and CF; therefore, the generated topography in these regions, such as the watershed boundary, surface slope and other characteristic parameters, could be extracted more easily by DEM data.

5 These results pose two significant scientific challenges for TMDLs. First, as model
uncertainty is difficult to quantify, the margin of safety (MOS) was often arbitrarily
assumed as 10% error. However, as shown in Table 4, this assumption is not highly
10 related to the reliability of the model system and supported the quantification of
TMDLs poorly. Specifically, compare to our previous studies (Shen et al., 2012b),
the uncertainties caused by input errors were greater than those resulting from model
parameters in 2001, 2005, and 2007, whereas uncertainties caused by inputs were
lower in the remaining years. Overall, the mean CV (0.168) for input-induced TP
uncertainty was slightly higher than that (0.156) for the parameter uncertainty, which
15 agrees with previous studies (Kuczera et al., 2006). Therefore, input data uncertainty is
critical in NPS modeling and efforts should be made to reduce this type of uncertainty.
Second, as illustrated in Fig. 3, the input data-induced uncertainty varies considerably
temporally and spatially as a complex function of climate, underlying topography, land
use, soil type, and management (Shen and Zhao, 2010; Chen et al., 2012). In this
sense, a site-specific MOS might be more robust to any particular sequence of input
20 errors than current steady MOS.

5 Conclusions

In this research, the impacts of four different input data types, including rainfall data,
DEMs, land use maps, and amount of fertilizer, on NPS modeling were quantified
and compared. Based on the results, input data-induced uncertainty is critical in NPS
25 modeling and efforts should be made to decrease this type of uncertainty. For the
case study, the mean CV value ranged from 0.101 to 0.271, which is slightly higher
than that for the parameter uncertainty. The study indicated that rainfall input resulted

11435

in the highest uncertainty, followed by DEM, land use maps, and fertilizer amount.
Therefore, measures should be taken first to reduce this source of uncertainty by
adding rain gauges, modifying the selection mechanism of rain gauge in SWAT, and
using appropriate interpolation techniques. This paper also demonstrated the required
5 input information would be reached if several key rain gauges and moderate-resolution
DEMs are used. This paper provides valuable information for developing TMDLs in
the Three Gorges Reservoir Area, and these results are also valuable to other model-
based watershed studies for the control of model uncertainty.

10 However, this conclusion might be only appropriate for NPS-TP and not for other
pollutants, i.e., the generation and transportation of nitrogen differ substantially from
those of NPS-P. Furthermore, the influence of soil type maps was not analyzed,
because only one coarse soil map was available for the study region. More researches
are needed if detailed input data sets are collected.

Data availability

15 The data could be obtained by emailing the first author.

Author contributions. Z. Shen designed the experiments. L. Chen and Y. Gong developed
the SWAT model and performed the simulations. L. Chen prepared the manuscript with
contributions from all co-authors.

20 *Acknowledgement.* This project was supported by the Fund for Innovative Research Group
of the National Natural Science Foundation of China (Grant No. 51421065), the National
Natural Science Foundation of China (No. 51409003 & 51579011), and Project funded by China
Postdoctoral Science Foundation.

11436

References

- Abbaspour, K. C., Yang, J., Maximov, I., Siber, R., Bogner, K., Mieleitner, J., Zobrist, J., and Srinivasan, R.: Modelling hydrology and water quality in the pre-alpine/alpine Thur watershed using SWAT, *J. Hydrol.*, 333, 413–430, 2007.
- 5 Andréassian, V., Perrin, C., Michel, C., Usart-Sanchez, I., and Lavabre, J.: Impact of imperfect rainfall knowledge on the efficiency and the parameters of watershed models, *J. Hydrol.*, 250, 206–223, 2001.
- Arnold, J. G., Srinivasan, R., Mutiah, R. S., and Williams, J. R.: Large area hydrologic modeling and assessment – Part 1: Model development, *J. Am. Water Resour. As.*, 34, 73–89, 1998.
- 10 Bárdossy, A. and Das, T.: Influence of rainfall observation network on model calibration and application, *Hydrol. Earth Syst. Sci.*, 12, 77–89, doi:10.5194/hess-12-77-2008, 2008.
- Beven, K.: A manifesto for the equifinality thesis, *J. Hydrol.*, 320, 18–36, 2006.
- Brazier, R. E., Heathwaite, A. L., and Liu, S.: Scaling issues relating to phosphorus transfer from land to water in agricultural catchments, *J. Hydrol.*, 304, 330–342, 2005.
- 15 Chaplot, V., Saleh, A., and Jaynes, D. B.: Impact of DEM mesh size and soil map scale on SWAT runoff sediment and NO₃-N loads predictions, *J. Hydrol.*, 312, 207–222, 2005.
- Chaubey, I., Cotter, A., Costello, T., and Soerens, T.: Effect of DEM data resolution on SWAT output uncertainty, *Hydrol. Process.*, 19, 621–628, 2005.
- Chen, D., Dahlgren, R. A., Shen, Y., and Lu, J.: A Bayesian approach for calculating variable total maximum daily loads and uncertainty assessment, *Sci. Total Environ.*, 430, 59–67, 2012.
- Chen, L., Zhong, Y., Wei, G., Cai, Y., and Shen, Z.: Development of an integrated modeling approach for identifying multilevel non-point-source priority management areas at the watershed scale, *Water Resour. Res.*, 50, 4095–4109, 2014.
- 25 Cotter, A., Chaubey, I., Costello, T., Soerens, T., and Nelson, M.: Water quality model output uncertainty as affected by spatial resolution of input data, *J. Am. Water Resour. As.*, 39, 977–986, 2003.
- Dixon, B. and Earls, J.: Resample or not?! Effects of resolution of DEMs in watershed modeling, *Hydrol. Process.*, 23, 1714–1724, 2009.
- 30 Duncan, M., Austin Bfabry, F., and Austin, G.: The effect of gauge sampling density on the accuracy of streamflow prediction for rural catchments, *J. Hydrol.*, 142, 445–476, 1993.

11437

- Han, J. C., Huan, G. H., Zhang, H., Li, Z., and Li, Y. P.: Bayesian uncertainty analysis in hydrological modeling associated with watershed subdivision level: a case study of SLURP model applied to the Xiangxi River watershed, China, *Stoch. Env. Res. Risk A.*, 28, 973–989, 2014.
- 5 Kuczera, G., Kavetski, D., Franks, S., and Thyer, M.: Towards a Bayesian total error analysis of conceptual rainfall–runoff models: characterising model error using storm-dependent parameters, *J. Hydrol.*, 331, 161–177, 2006.
- Lin, S., Jing, C., Coles, N. A., Moore, N., and Wu, J.: Evaluating DEM source and resolution uncertainties in the Soil and Water Assessment Tool, *Stoch. Env. Res. Risk A.*, 27, 209–221, 2013.
- 10 Liu, Y. and Gupta, H.: Uncertainty in hydrologic modeling: toward an integrated data assimilation framework, *Water Resour. Res.*, 43, W07401, doi:10.1029/2006WR005756, 2007.
- Mango, L. M., Melesse, A. M., McClain, M. E., Gann, D., and Setegn, S. G.: Land use and climate change impacts on the hydrology of the upper Mara River Basin, Kenya: results of a modeling study to support better resource management, *Hydrol. Earth Syst. Sci.*, 15, 2245–2258, doi:10.5194/hess-15-2245-2011, 2011.
- 15 McMillan, H., Jackson, B., Clark, M., Kavetski, D., and Woods, R.: Rainfall uncertainty in hydrological modelling: An evaluation of multiplicative error models, *J. Hydrol.*, 400, 83–94, 2011.
- 20 Moriasi, D. N., Arnold, J. G., Van Liew, M. W., Bingner, R. L., Harmel, R. D., and Veith, T. L.: Model evaluation guidelines for systematic quantification of accuracy in watershed simulations, *T. ASABE*, 50, 885–900, 2007.
- Munoz-Carpena, R., Vellidis, G., Shirmohammadi, A., and Wallender, W. W.: Evaluation of modeling tools for TMDL development and implementation, *T. ASABE*, 49, 961–965, 2006.
- 25 Pai, N. and Saraswat, D.: Impact of land use and land cover categorical uncertainty on SWAT hydrologic modeling, *T. ASABE*, 56, 1387–1397, 2013.
- Payraudeau, S., Cernesson, F., Tournoud, M. G., and Beven, K. J.: Modelling nitrogen loads at the catchment scale under the influence of land use, *Phys. Chem. Earth*, 29, 811–819, 2004.
- 30 Schuurmans, J. M. and Bierkens, M. F. P.: Effect of spatial distribution of daily rainfall on interior catchment response of a distributed hydrological model, *Hydrol. Earth Syst. Sci.*, 11, 677–693, doi:10.5194/hess-11-677-2007, 2007.

11438

- Seibert, J. and Beven, K. J.: Gauging the ungauged basin: how many discharge measurements are needed?, *Hydrol. Earth Syst. Sci.*, 13, 883–892, doi:10.5194/hess-13-883-2009, 2009.
- Shen, J. and Zhao, Y.: Combined Bayesian statistics and load duration curve method for bacteria nonpoint source loading estimation, *Water Res.*, 44, 77–84, 2010.
- 5 Shen, Z. Y., Chen, L., Liao, Q., Liu, R. M., and Hong, Q.: Impact of spatial rainfall variability on hydrology and nonpoint source pollution modeling, *J. Hydrol.*, 472, 205–215, 2012a.
- Shen, Z. Y., Chen, L., and Chen, T.: Analysis of parameter uncertainty in hydrological and sediment modeling using GLUE method: a case study of SWAT model applied to Three Gorges Reservoir Region, China, *Hydrol. Earth Syst. Sci.*, 16, 121–132, doi:10.5194/hess-16-121-2012, 2012b.
- 10 Shen, Z. Y., Chen, L., Liao, Q., Liu, R. M., and Huang, Q.: A comprehensive study of the effect of GIS data on hydrology and non-point source pollution modeling, *Agr. Water Manage.*, 118, 93–102, 2013.
- Strauch, M., Bernhofer, C., Koide, S., Volk, M., Lorz, C., and Makeschin, F.: Using precipitation data ensemble for uncertainty analysis in SWAT streamflow simulation, *J. Hydrol.*, 414–415, 413–424, 2012.
- 15 Van Griensven, A., Meixner, T., Grunwald, S., Bishop, T., Diluzio, A., and Srinivasan, R.: A global sensitivity analysis tool for the parameters of multi-variable catchment models, *J. Hydrol.*, 324, 10–23, 2006.
- Wellen, C., Arhonditsis, G. B., Labencki, T., and Boyd, D.: Application of the SPARROW model in watersheds with limited information: a Bayesian assessment of the model uncertainty and the value of additional monitoring, *Hydrol. Process.*, 28, 1260–1283, 2014.
- Wu, S., Li, J., and Huang, G. H.: An evaluation of grid size uncertainty in empirical soil loss modeling with digital elevation models, *Environ. Model. Assess.*, 10, 33–42, 2005.
- 25 Wu, S., Li, J., and Huang, G. H.: Modeling the effects of elevation data resolution on the performance of topography-based watershed runoff simulation, *Environ. Modell. Softw.*, 22, 1250–1260, 2007.
- Xue, C., Chen, B., and Wu, H.: Parameter uncertainty analysis of surface flow and sediment yield in the Huolin Basin, China, *J. Hydrol. Eng.*, 19, 1224–1236, 2014.
- 30 Zhang, P., Liu, R., Bao, Y., Yu, W., and Shen, Z.: Uncertainty of SWAT model at different DEM resolutions in a large mountainous watershed, *Water Resour.*, 53, 132–144, 2014.

11439

- Zheng, Y., Wang, W., Han, F., and Ping, J.: Uncertainty assessment for watershed water quality modeling: a Probabilistic Collocation Method based approach, *Adv. Water Resour.*, 34, 887–898, 2011.

11440

Table 3. The values of E_{NS} and R^2 of the SWAT model during the calibration and validation period.

Variable	Indicator	Calibration	Validation
Flow	E_{NS}	0.66	0.89
	R^2	0.79	0.95
Sediment	E_{NS}	0.73	0.67
	R^2	0.83	0.83
TP	E_{NS}	0.75	0.13
	R^2	0.86	0.79

11443

Table 4. The sensitivity of simulated TP (CV values) to different input dataset.

Input data	2000	2001	2002	2003	2004	2005	2006	2007	Mean
Single gauge	0.419	0.421	0.332	0.587	0.319	0.417	0.284	0.410	0.388
Multi-gauges	0.433	0.362	0.240	0.287	0.141	0.256	0.098	0.241	0.249
NFGIS DEM	0.026	0.119	0.059	0.025	0.026	0.043	0.105	0.040	0.056
ASTER GDEM	0.189	0.276	0.225	0.105	0.198	0.255	0.383	0.274	0.197
Land use maps	0.022	0.013	0.018	0.018	0.024	0.036	0.009	0.024	0.027
Fertilizer amount	0.004	0.003	0.003	0.003	0.006	0.007	0.003	0.005	0.005
Input uncertainty	0.151	0.208	0.116	0.101	0.112	0.271	0.141	0.246	0.168
Parameter uncertainty	0.167	0.145	0.177	0.141	0.147	0.151	0.154	0.164	0.156

11444

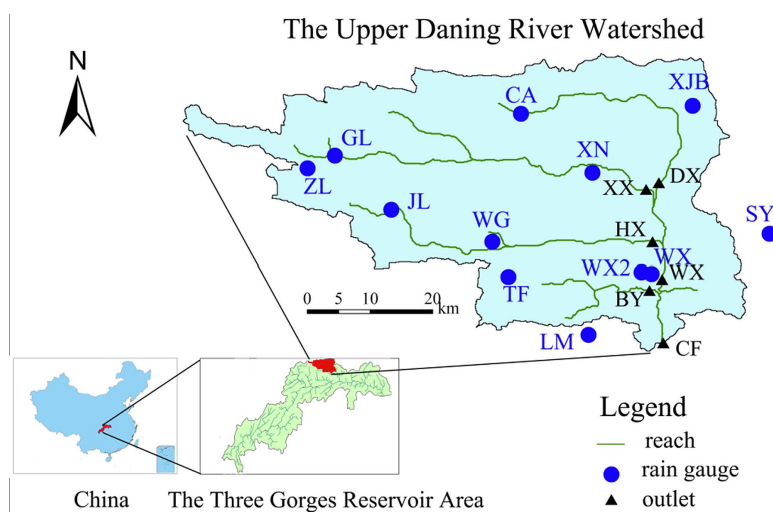


Figure 1. Locations of and the rain gauges within the Upper Daning River Watershed.

11445

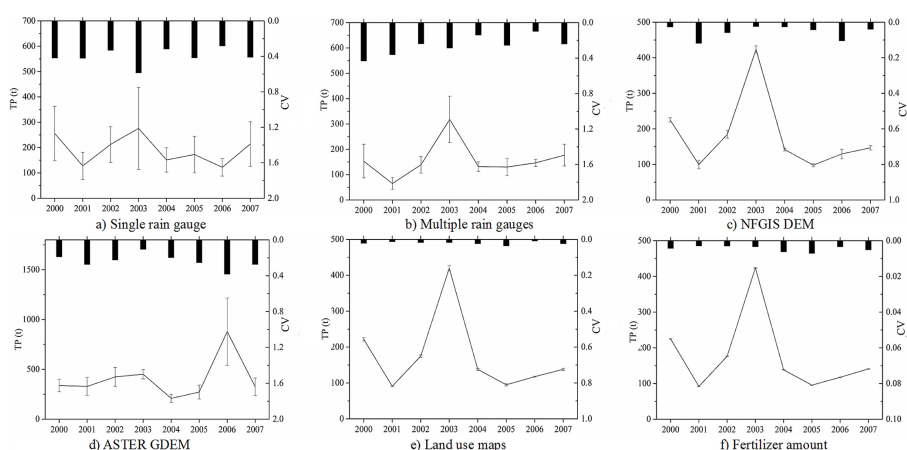


Figure 2. Uncertainty of simulated TP induced by each input data, in which the line, error bar and inverted column indicate the mean value, SD and CV values, respectively.

11446

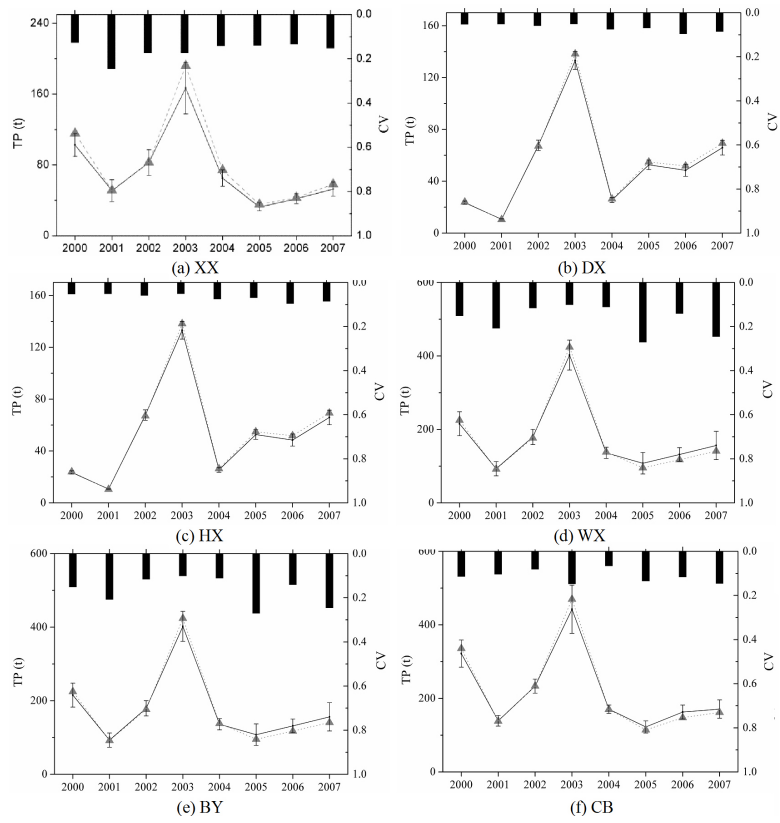


Figure 3. Comprehensive uncertainty of input data-induced simulated TP, in which the line, error bar and inverted column indicate the mean value, SD and CV values, respectively.